

Image Cover Sheet

CLASSIFICATION

UNCLASSIFIED

SYSTEM NUMBER

506950



TITLE

FINITE ELEMENT COMPARATIVE STUDY OF SHIP STRUCTURAL DETAIL

System Number:

Patron Number:

Requester:

Notes:

DSIS Use only:

Deliver to:



Finite Element Comparative Study of Ship Structural Detail

Y. Iwahashi,^a Y. Sumi,^b T. Hu,^c H. Paetzold,^d C. C. Wu,^e C. D. Jang,^f

P. Rigo,^g W. Nie,^h and H. Kawanoⁱ

^a Research & Development Center, Sumitomo Heavy Industries, Ltd., Hiratsuka,
Japan

^b Department of Naval Architecture and Ocean Engineering, Yokohama National
University, Yokohama, Japan

^c Defence Research Establishment Atlantic, Dartmouth, Canada

^d Institute of Naval Architecture, University of Hamburg, Hamburg, Germany

^e United Ship Design & Development Center, Keelung, Taiwan, China

^f Department of Naval Architecture and Ocean Engineering, Seoul National
University, Seoul, Korea

^g Naval Architecture and Transport Systems Department, University of Liege, Liege,
Belgium

^h Department of Naval Architecture and Ocean Engineering, Harbin Engineering
University, Harbin, China

ⁱ Nagasaki Research & Development Center, Mitsubishi Heavy Industries, Ltd.,
Nagasaki, Japan

Abstract

A comparative study of the finite element analysis of the local stresses in a ship structural detail has been carried out by the members of Technical Committee 1 of ISSC '97. An experimental model for the intersection structure of longitudinal stiffeners and a transverse frame was selected as the analysis object. Finite element analysis results of eight shell element models and one solid element model were collected for this comparative study. It is found that the results of shell element models for local stresses have high correlation with each other, but give significantly lower stresses than the experimental results. The results of the solid element model, on the other hand, agreed well with the experimental results at the weld toe. A possible interpretation of the results of shell element models, in the practical procedures of hot spot stress evaluation, is discussed.

Key words : comparative study, finite element structural analysis, hot spot stress

1 INTRODUCTION

For the evaluation of fatigue strength of ship structures, explicit fatigue analysis is becoming an important part of ship structural design. The hot spot stress approach, combined with detailed finite element analysis, is expected to be the most practical method. The concept of hot spot stresses, which has been often applied to the tubular

joints of offshore structures, is generally understood to be the stresses at weld toe locations taking into consideration all geometrical influences except for the local weld geometry. However, the calculated local stresses around the structural singularities vary depending on the structural idealization, the element types used and the mesh subdivisions. An increasing amount of work is now being carried out for the practical evaluation of hot spot stresses of stiffened plate structures. In order to obtain some standards or guidelines for the analysis, it was decided by Technical Committee ..1 of ISSC'97 to carry out a finite element comparative study focusing attention to the evaluation of hot spot stresses of ship structural details. The experimental model of research project SR219 in Japan was selected as the analysis model of the comparative study so that the calculated results could be compared with the experimental results for the proper validation.

2 EXPERIMENTAL MODEL

The stiffened panel test model, shown in Fig. 1, is for a part of a typical side longitudinal and transverse bulkhead intersection of crude oil tankers. The model consists of three longitudinal stiffeners and one transverse frame, and has twofold symmetry with respect to longitudinal and transverse directions, respectively. The transverse frame is supported by tripping brackets at the center longitudinal and stiffened by flat bars at the side longitudinals. The model is made of high strength hull

structural steel of class KA32 having the yield strength higher than 314 MPa (32 Kgf/mm²), and constructed applying the same welding procedure as used for actual ship structures.

The load is applied in a three point bending configuration in the horizontal direction, using a hydraulic actuator, through the triangular loading plate of 40 mm thickness attached to the flange plate of the transverse frame. The model was supported at vertical reaction columns through rollers at the ends of longitudinals. While increasing the loads gradually from zero to a maximum of 392 kN (40 tonf), displacements and strains were measured at several reference points and critical locations. Uni-axial strain gauges were used to measure the longitudinal strain components. At the weld joint of the side longitudinal flange plate and the flat bar stiffener, which is expected to be the location of first fatigue crack initiation, stress concentration gauges were used to evaluate the hot spot stresses. Measuring points, used for the comparison with the analysis results, are shown in Fig. 2.

3 ANALYSIS MODELS

Nine analysis models, shown in Table 1, were collected for this comparative study from seven committee members and one outside collaborator. Mesh divisions for some of the models are illustrated in the Appendix.

The problem was analyzed independently by each contributor using his own solution procedures, based on the following common guidelines,

- (1) Solution method is to be the linear elastic analysis;
- (2) Material properties for the ship structural steel is to be isotropic linear elastic with Young's modulus = 206GPa, Poisson's ratio = 0.3; and
- (3) Magnitude of applied load to be 392 kN (40 tonf).

No information concerning the experimental results was given prior to the analysis.

All the participants made use of the twofold symmetry condition, and the quarter part of the test model was analyzed. Only one model, model (3), was constructed using three dimensional solid elements, while all the other models were idealized using shell elements, where the detailed geometry of the weld was not represented. Graded mesh divisions were applied, except for model (8), with the element size on the order of one plate thickness near the transverse/longitudinal connections. In model (8), relatively uniform fine mesh divisions were used over the zooming model for 1/12 of the structure on 1200 mm length.

4 COMPARISON OF FINITE ELEMENT ANALYSIS RESULTS

Finite element analysis results are compared in Table 1, together with the experimental results and results obtained by hand calculation based on beam theory. Numerical values of measured stresses were obtained multiplying the measured strains by E (Young's Modulus = 206 GPa) . Variations of the measured results at symmetrical locations with respect to longitudinal and transverse directions were generally small, several percent on average and 5% at the most.

The experimental value of the deflection in Table 1, obtained from the measured relative displacement between the center and supporting points of the center longitudinal, was slightly smaller than predicted by the analyses. A likely reason for this difference is the slightly non-linear behavior of the load displacement relation observed in the experiment at lower load levels, which could be caused by the effects of the local deformation at the contact points of the supporting rollers and the loading apparatus rigidity.

Table 1 includes the stress results of reference sections at 800 mm from the center of the model, at the bracket end section of the center longitudinal and at the stiffener end section of the side longitudinal. The average of calculated stresses are plotted versus experimental stresses in Fig. 3. Excellent correlation between the analysis and experimental results can be observed except for the region close to the weld toe (E21, E40). The coefficient of variation (COV) of the analysis results are shown in Fig. 4. It can be observed that the COV has a tendency to decrease with the increase of stresses except at the bracket and the stiffener weld toe (E21, E40).

As for the determination of hot spot stresses at the weld toe, several different methods of extrapolation have been proposed. Hence, it was decided that the comparison of the analysis results will be made on the stress distribution near the welded joint, rather than on the hot spot stress itself. The results for the stress distribution of the flange plate of the side longitudinal near the stiffener weld toe end are shown in Fig. 5. It is interesting to note that the results using shell elements have high correlation with each other, but give significantly lower stresses than the

experimental results. The results of the solid element model (3), on the other hand, agree well with the experimental results at the weld toe. Since the number of results of solid element models available for comparison is limited, a supplemental analysis was carried out using solid elements to confirm the results of model (3). The additional results are shown in Fig. 5 as (10) and a good agreement with the results of model (3) is observed.

5 DISCUSSION

Since all the shell element models do not include the weld, the difference between the calculation results and the experiment may be attributed to the effects of weld geometry. Fricke & Paetzold¹ pointed out the importance of proper modeling of exact fillet weld stiffness. It is also pointed out by Kawano et al.² that shell element models sometimes give lower estimates for stress concentration due to the effect of the plate thickness. Although the number of experimental measurements and the types of the structure investigated are limited in the present comparative study, it can be concluded that the solid element model including weld geometry is recommended especially when the correlation with experimental results is to be pursued.

However, considering the expensive analysis cost of the solid element model, it is also important to establish a reliable and practical procedure based on shell element idealization for hot spot stress estimation. It should be noted that some of the contributors with shell element models used extremely fine meshes at the area of

stress concentration, but the variations of the results remained relatively small. This indicates that the shell element model could be used as a reliable tool in the design analyses. In order to avoid the underestimation of stress concentration by the shell element models, however, some modification or interpretation have to be considered.

Machida et. al. ³ proposed to include geometrical effects of weld connections into the shell element idealization by increasing the element plate thickness by about half the weld leg length.

In the DNV procedure⁴ for hot spot stress evaluation, the hot spot for shell element models, which do not include the weld, is located not at the weld toe but at the element intersection lines, and the stresses at a distance $0.5t$ and $1.5t$ from this intersection line are used for the extrapolation, where t is the plate thickness. A similar procedure to shift the stress distribution is used in NK Guidance ⁵. These practical procedures for hot spot stress evaluation, validated by experimental and analytical studies, are important for the accurate fatigue life estimation of ship structural details.

..CONCLUSIONS

A finite element comparative study of a ship structural detail was carried out with eight shell element models and one solid element idealization, focusing attention on the hot spot stress evaluation at weld connections. From the comparison of analysis and experimental results, it can be concluded that

(1) Three dimensional solid element models which include the representation of the

weld geometry are recommended for the precise prediction of local stresses at weld connections.

- (2) Shell element models can be used as a reliable tool for design analyses. However, if the weld is not included in the model, some interpretation of the results to avoid under estimation have to be introduced such as to shift the stress distribution from the element intersection line to the weld toe.

Practical procedures to precisely predict local stress distributions, validated by experiments as in the above, are expected to contribute to the design of reliable ship structures.

ACKNOWLEDGMENT

The authors wish to thank the Research Committee, SR219 (Chairman, Professor S. Machida, The University of Tokyo) of the Shipbuilding Research Association of Japan for permitting the use of the experimental data which made it possible to carry out the present FEA comparative study. Acknowledgement is also made to Mr J. Waegter (Ramboll A/S), Mr. R. Loseth (Det norske Veritas) and Dr. W. Fricke (Germanischer Lloyd) for their valuable discussions.

REFERENCES

1. Fricke, W. and Paetzold, H. Fatigue Strength Assessment of Scallops – an Example for the Application of Nominal and Local Stress Approaches, *Marine Structures* 8 (1995), pp.423-447
2. Kawano, H., K. Satoh and Y. Taguchi (1994). Basic Study on Fatigue Strength Evaluation (second report : SN diagram to structural details from a viewpoint of attaining FEM direct strength calculation) *Jnl of Soc of Naval Architects of Japan*, Vol 176, pp409-415
3. Machida, S, M. Matoba, H. Yoshinari and R. Nishimura (1992) Definition of Hot Spot Stress in Welded Plate Type Structure for Fatigue Assessment (3rd Report), *Jnl of Soc of Naval Architects of Japan*, Vol 171, pp477-484
4. Cramer, E. , S. Gran, G. Holtsmark, I. Lotsberg, R. Loeth, K. Olaisen and S. Valsgard (1995) Fatigue Assessment of Ship Structures, Technical Report 93-0432, Det Norske Veritas
5. NK (1996) Guidance for Fatigue Design of ship structures, Nippon Kaiji Kyokai

MODEL	EXP	BEAM	(1)	(2)	(3)	(4)	(5)	(6)	(7)	(8)	(9)	AVERAGE	COV
element			shell	shell	solid	shell	shell	shell	shell	shell	shell		
Num of DOF			1,904×6	2,109×6	30,400	1,294×6	1,231×6	1,231×6	2,640×6	2,640×6			
solver			ALGOR	NASTRAN	MARC	NASTRAN	ANSYS	ANSYS	NASTRAN	MSLHCN			
pre-post			ALGOR	PATRAN	MENTAT	I-DEAS	ANSYS	ANSYS	PATRAN				
DEFLECTION (mm)	4.63	4.89	4.91	4.99	5.02	5.62	5.64	4.59	5.22	4.06	4.81	5.0	0.099
E19	80.2	83.4	86.8	83.9	88.2	89.8	83	77.7	88.4	81.4	89.9	85.5	0.049
E33	-26.3	-24.2	-28	-20.4	-28.4	-26.2	-21.8	-24	-24.8	-28.3	-28.8	-25.6	0.120
E20	95.3	99.8	94	97.2	102.3	102.3	101.2	107.1	97.6	94.5	112.5	101.0	0.060
E21	140.2	99.8	108.1	105.5	165.2	114.7	109.6	119.7	112	109	122	118.4	0.155
E22	95.3	99.8	94	97.2	102.3	102.3	101.2	107.1	97.6	94.5	112.5	101.0	0.060
E23	78.2	86.5	85.3	90	97.2	102.1	104.1	104		87	95.4	95.6	0.079
E24	26.7	34.7	31.6	38.6	31.2	33.2	35.4	39.3	31.4	25	27.3	32.6	0.145
E25	-19.3	-17.2	-22	-17.6	-26.7	-24.5	-22.1	-14.7	-28	-17.5	-23.8	-21.9	0.205
E34	-33.7	-30.5	-36.8	-25.4	-36.1	-30.8	-29.9	-29.7	-34.4	-34	-36.5	-32.6	0.119
E37	79.4	83.4	78.4	77.6	80.8	83	82.8	69.9	80.8	78.4	74.9	78.5	0.053
E55	-24.6	-25.5	-24.5	-18	-25.4	-23.9	-18.3	-21.2	-22.6	-27.3		-22.7	0.146
E38	111.3	113.0	104.9	106.9	110.6	116.5	115.8	98.8	101.4	108	98.6	106.8	0.062
E40	180.7	112.9	114.1	128.6	185.9	131.6	117.8	116.7	118.1	117	115.7	127.3	0.179
E44	107.0	113.0	104.5	106.6	109.9	116.2	98.6	78.4	101.1	108	98.8	102.5	0.104
E45	81.8	97.9	90.2	90.2	99.1	111	122.9	88.7		91	80.4	96.7	0.143
E46	30.1	39.2	33	37.6	33.6	36.5	46.4	28.2	31.4	30	28.9	34.0	0.167
E47	-21.4	-19.4	-23.7	-22.9	-29.9	-27.6	-22.4	-22.1	-28	-22	-23.8	-24.7	0.120
E56	-36.5	-34.6	-36.5	-28.2	-38.3	-37.7	-28.9	-33	-34.4	-37.1	-33.6	-34.2	0.108

Table 1 Comparison of Analysis Results

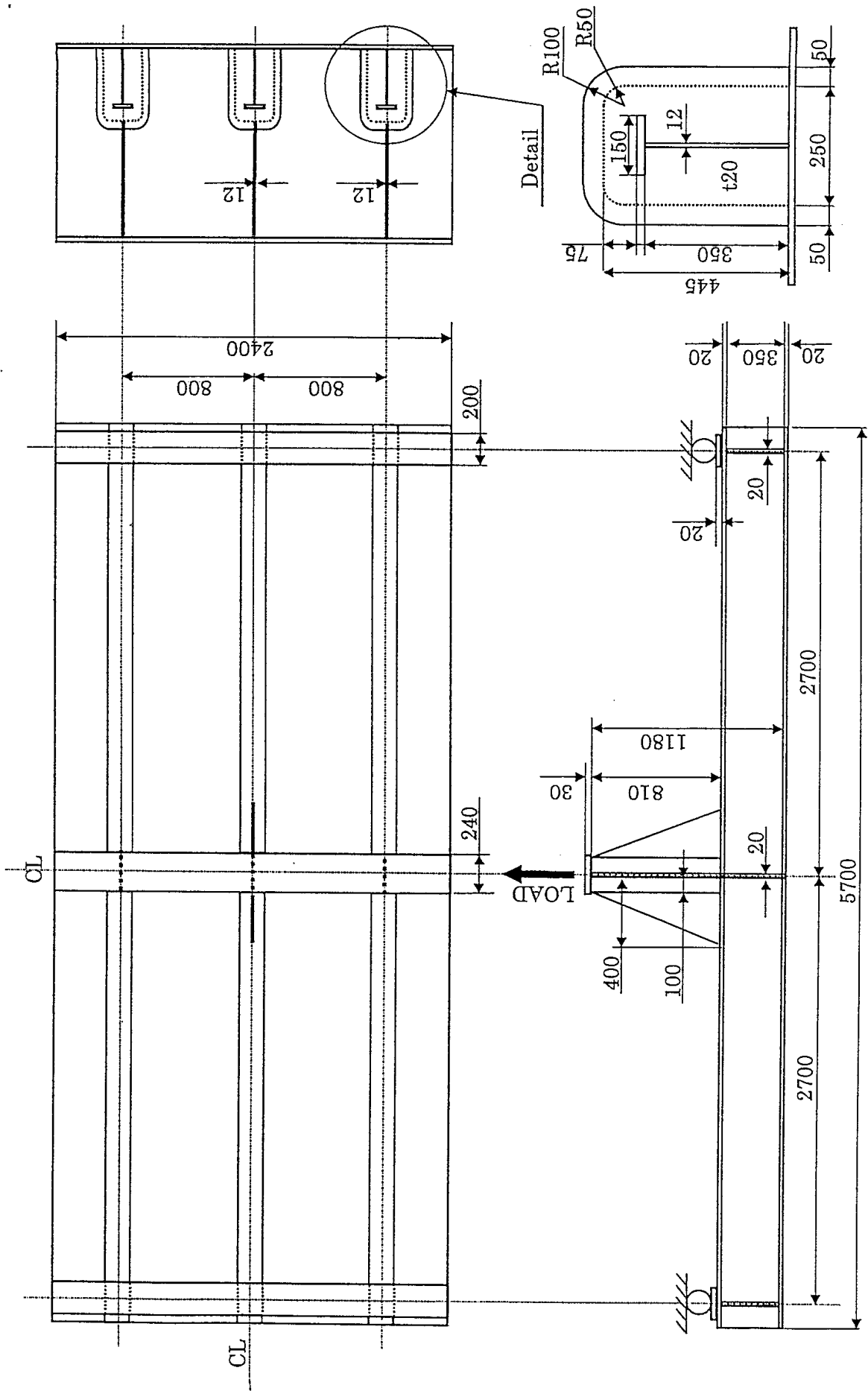


Fig. 1 Experimental Model

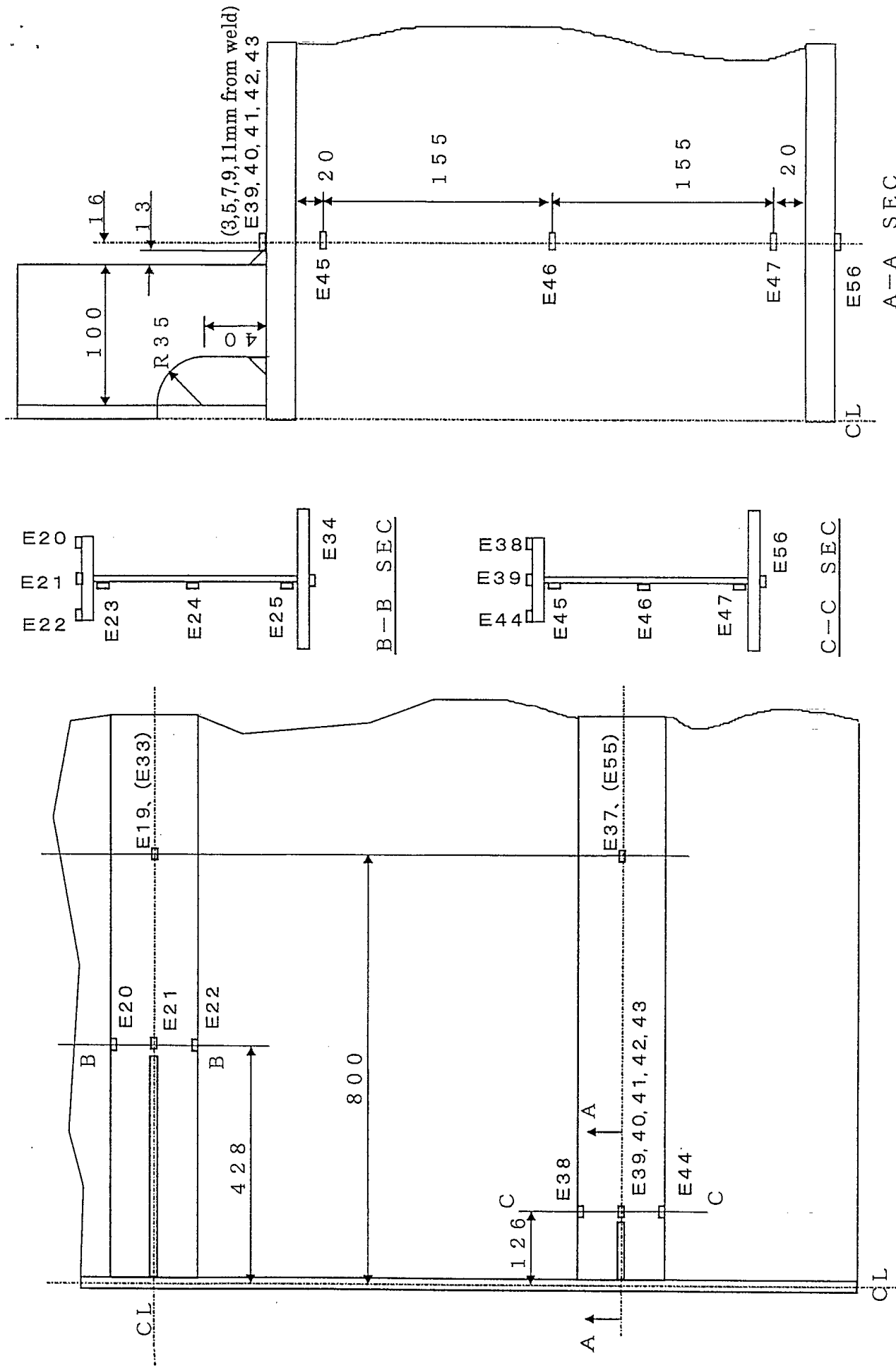


Fig.2 Strain Measurement Locations

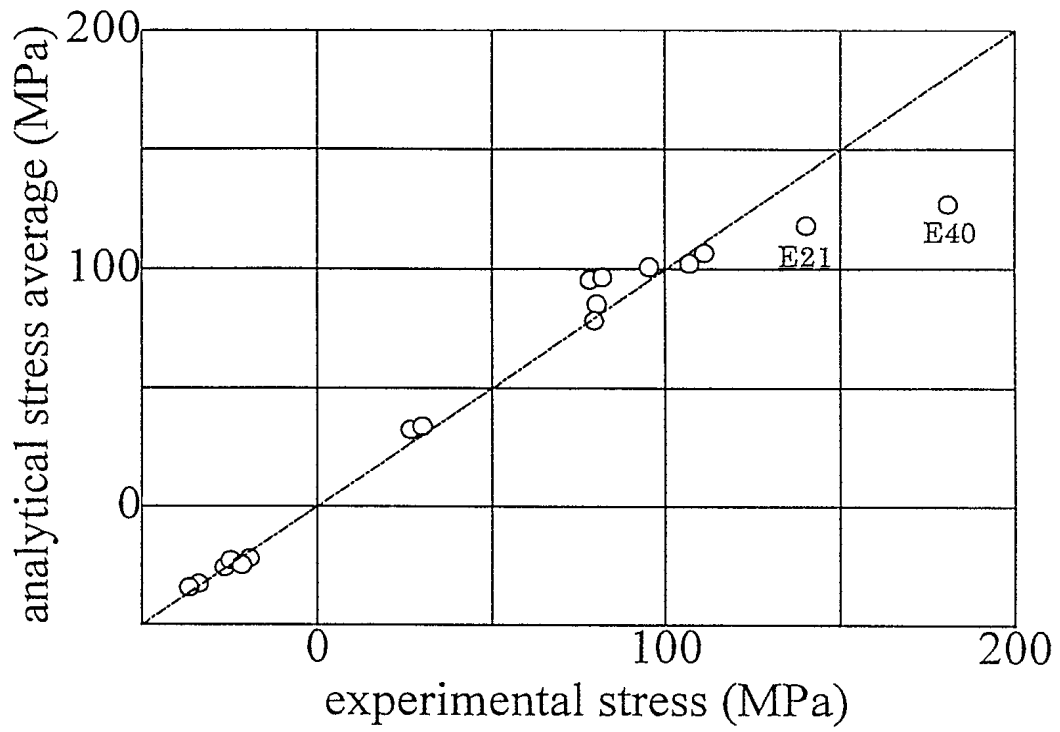


Fig. 3 Comparison with Experiment

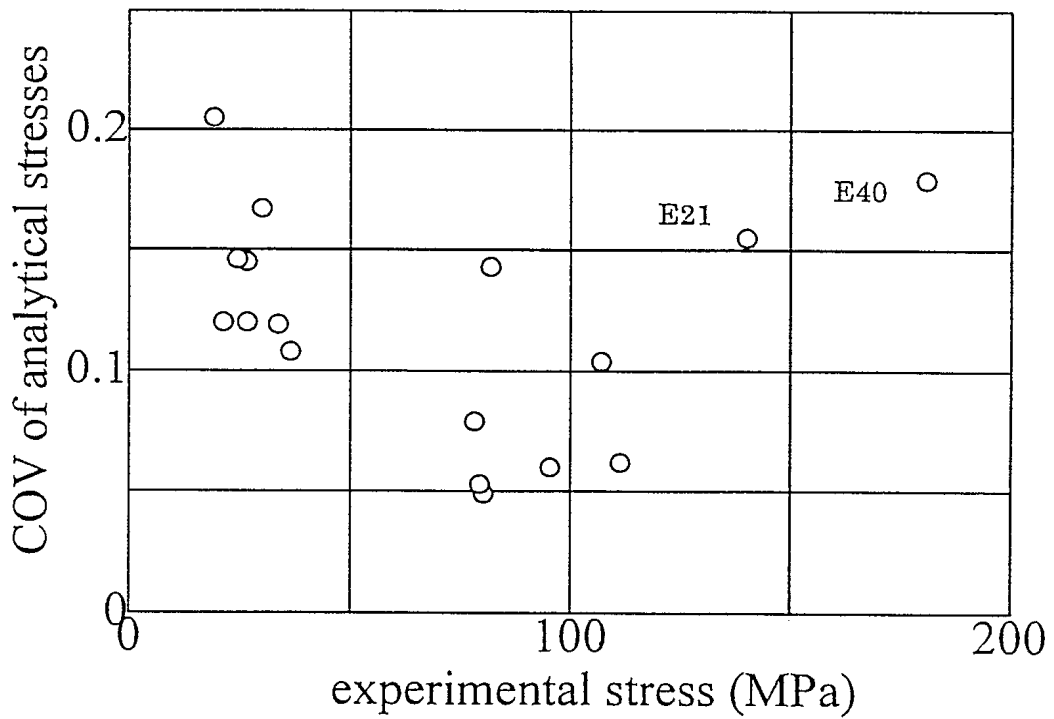


Fig. 4 Variation of Analysis Results

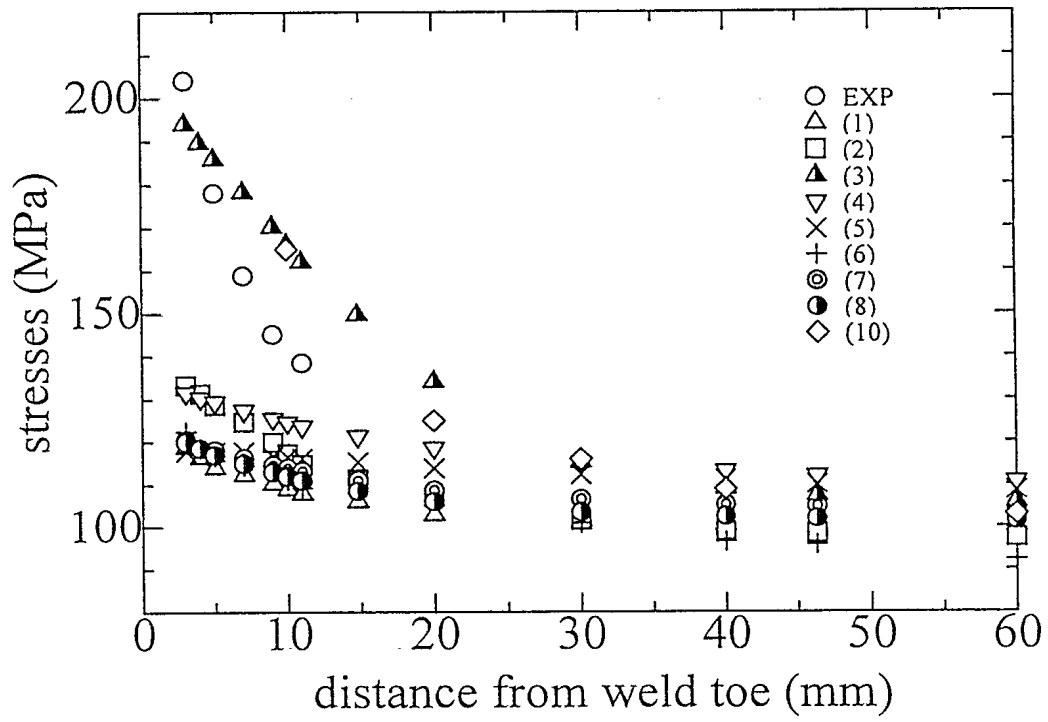


Fig.5 Stress Distribution at the Weld

APPENDIX

Mesh division of finite element models

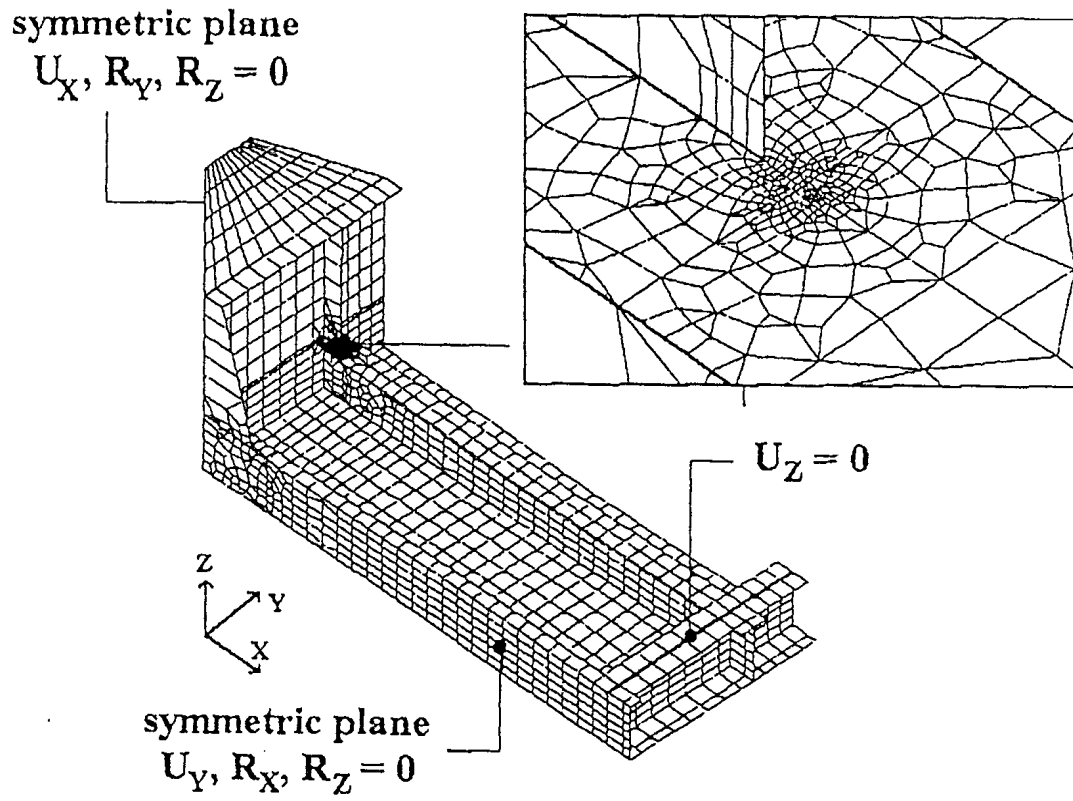


Fig. A.1 Mesh division of Model (1)

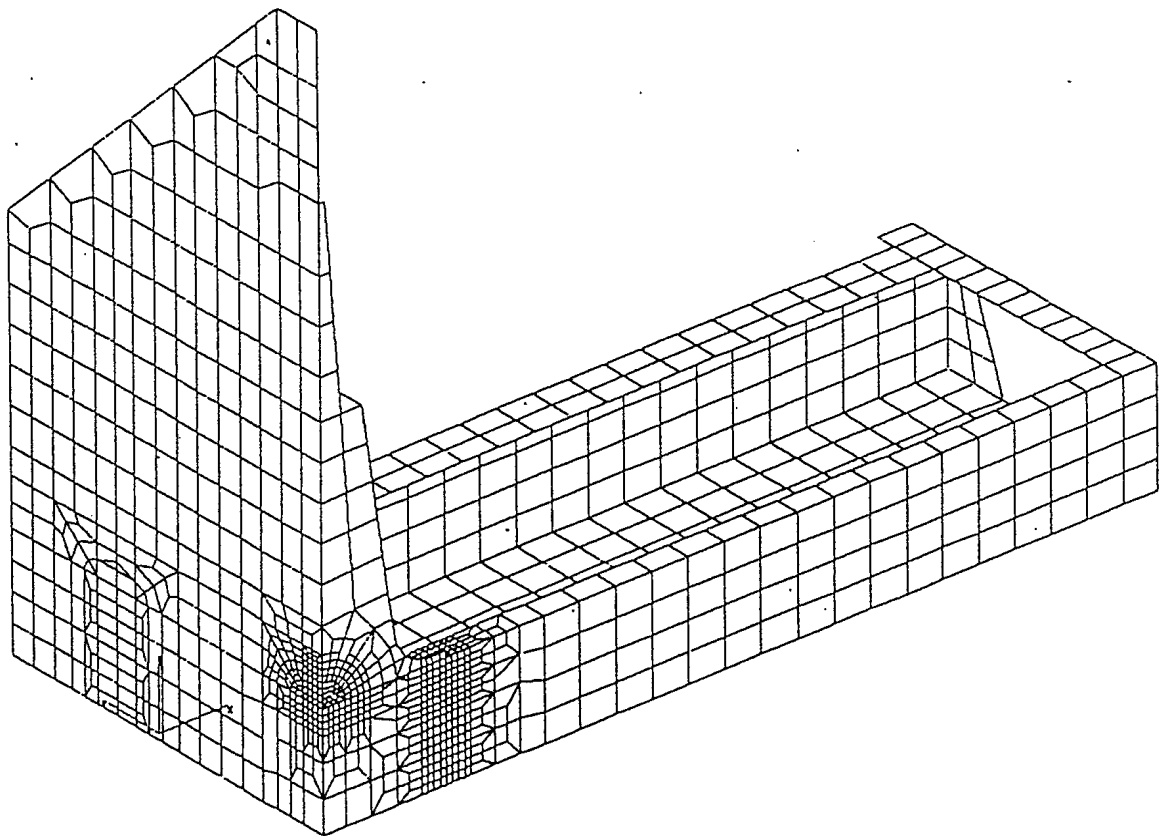


Fig. A.2 Mesh division of Model (2)

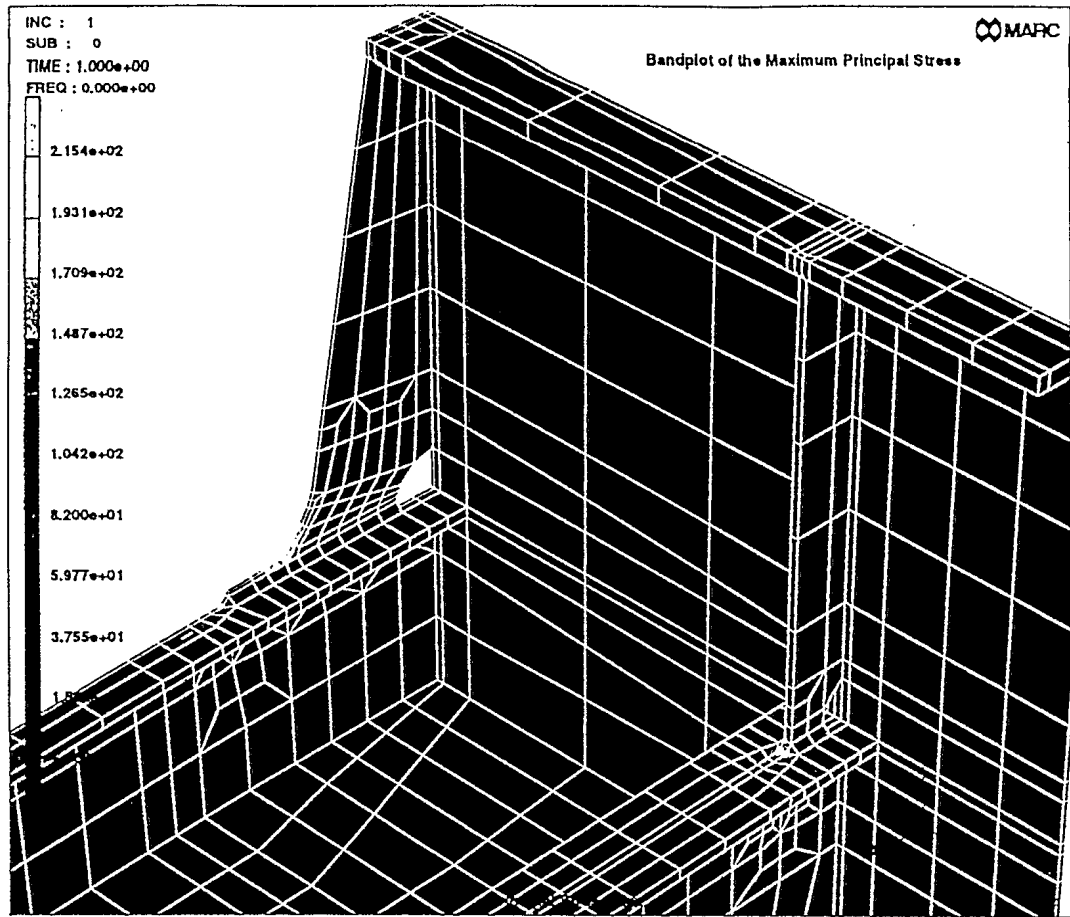


Fig. A.3 Mesh division of Model (3)

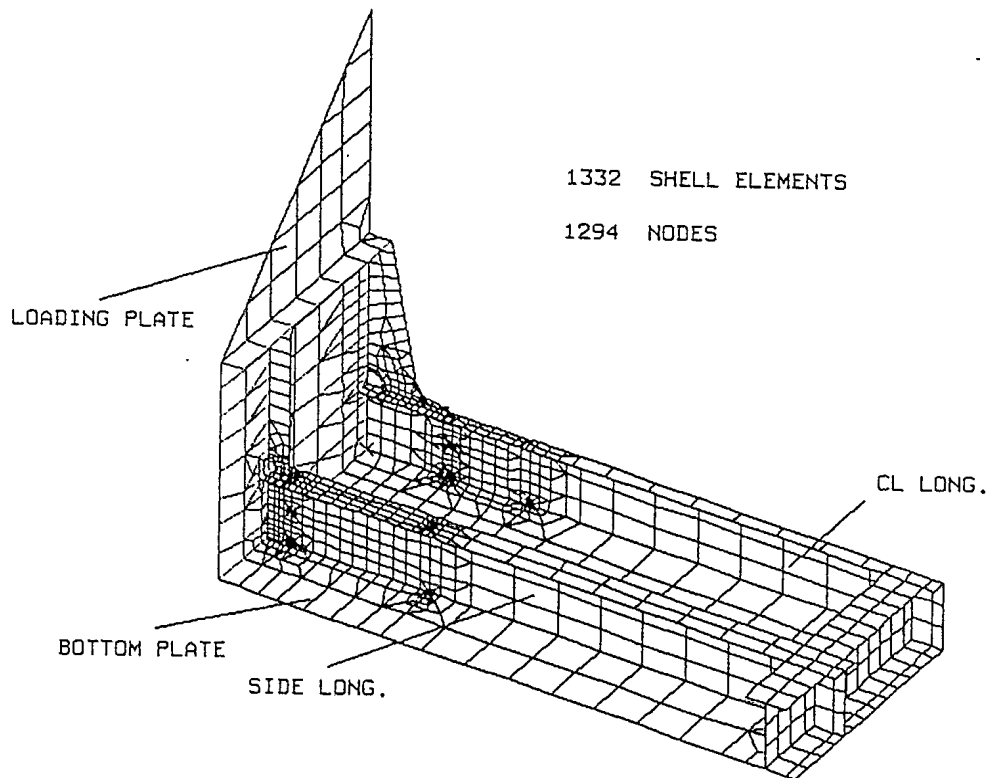


Fig. A.4 Mesh division of Model (4)

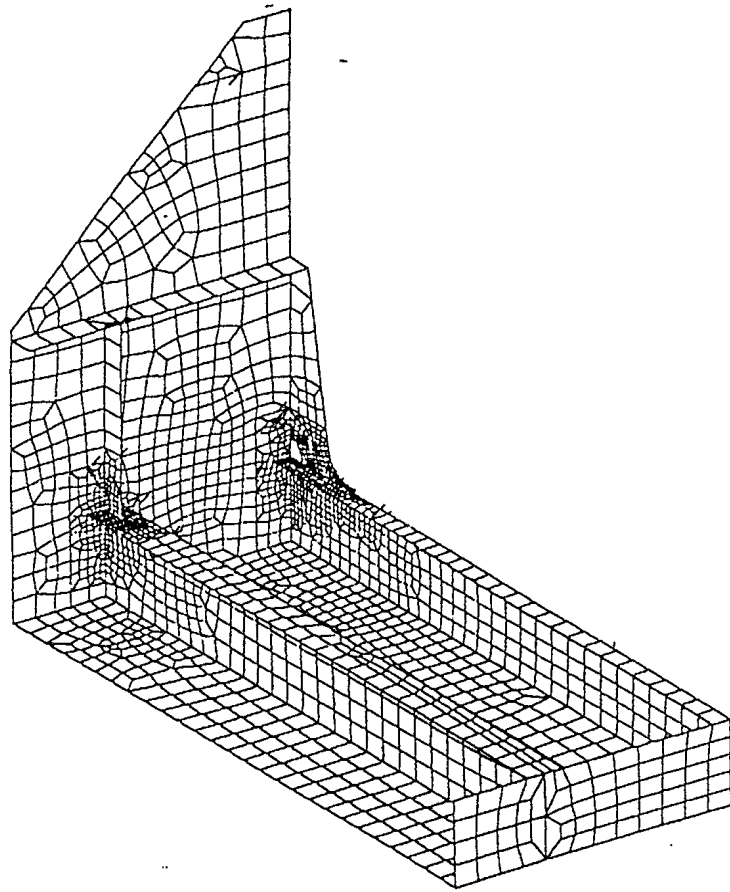


Fig. A.5 Mesh division of Model (5)

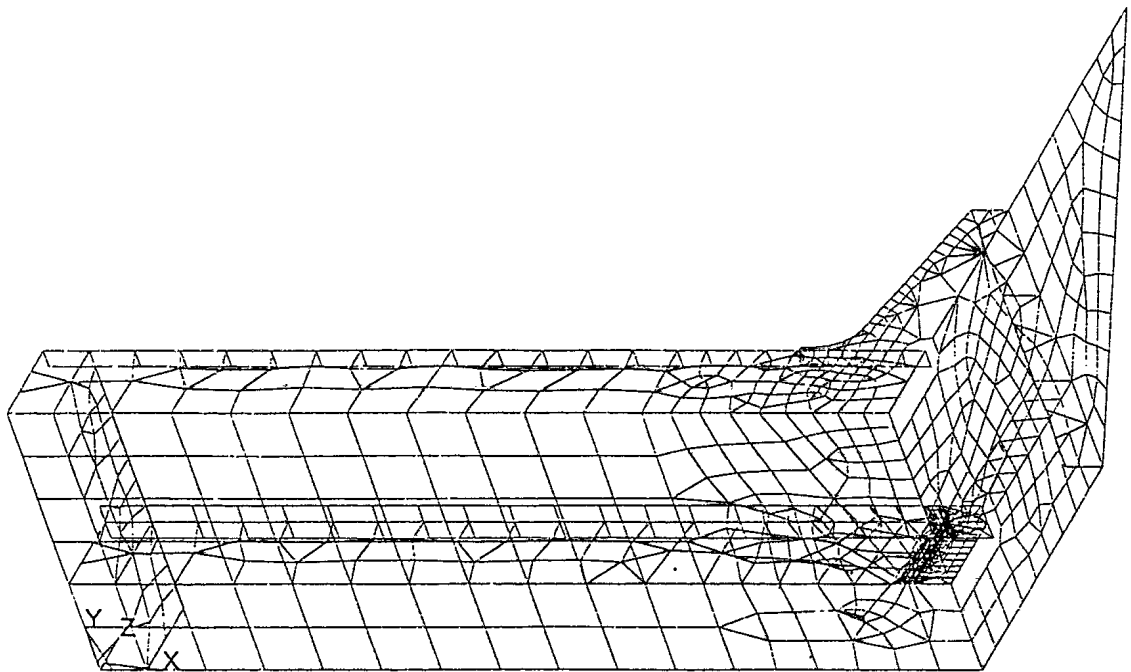


Fig. A.6 Mesh division of Model (6)

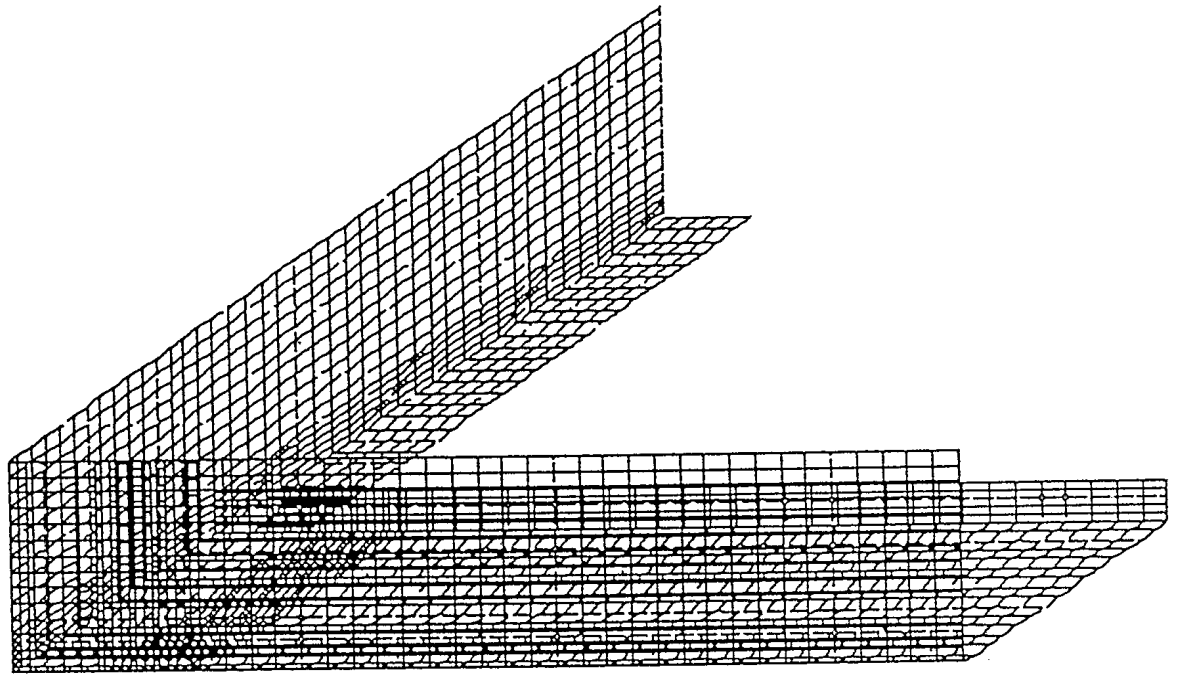


Fig. A.7 Mesh division of Model (8)

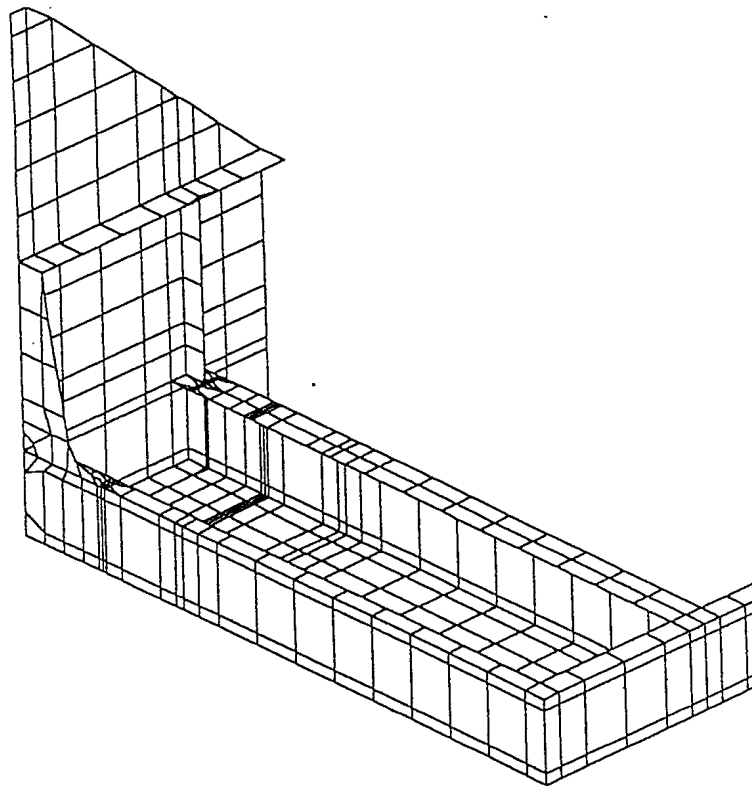


Fig. A.8 Mesh division of Model (9)

#506950